Severity of structural and functional right ventricular remodeling depends on training load in an experimental model of endurance exercise

Maria Sanz-de la Garza[1,2,#]; Cira Rubies[2,#]; Montserrat Batlle[2,3]; Bart H Bijnens[4,5]; Lluis Mont[1,2,3]; Marta Sitges[1,2,3]; and Eduard Guasch[1,2,3,*]

[1] Cardiovascular Institute, Hospital Clínic, Universitat de Barcelona, Barcelona, Catalonia, Spain.
[2] Institut d'Investigacions Biomédiques August Pi i Sunyer (IDIBAPS), Barcelona, Catalonia, Spain
[3] CIBERCV
[4] ICREA, Barcelona, Spain
[5] Universitat Pompeu Fabra, Barcelona, Spain.

# MS and CR contributed equally and share first authorship.

Running head: Exercise load modulates RV remodeling

*** To whom correspondence should be sent:**

Eduard Guasch
Cardiology Department; Cardiovascular Institute, Hospital Clínic
Villarroel 136, 08036 Barcelona, Spain
Phone +34-932275505; E-mail: eguasch@clinic.cat

ABSTRACT

An arrhythmogenic right ventricle (RV) remodeling has been reported in response to regular training, but it remains unclear how exercise intensity affects the presence and extent of such remodeling. We aimed at assessing the relationship between RV remodeling and exercise load in a long-term endurance training model. Wistar rats were conditioned to run at moderate (MOD, 45 min, 30cm/s) or intense (INT, 60 min, 60cm/s) workloads for 16 weeks; sedentary rats (SED) served as controls. Cardiac remodeling was assessed with standard echocardiographic and tissue Doppler techniques, sensor-tip pressure catheters and pressure-volume loop analyses. After MOD training, both ventricles similarly dilated (~16%); the RV apical segment deformation, but not the basal one, was increased (apical strain rate [SR] (s^{-1}): -2.9±0.5 vs -3.3±0.6, SED vs MOD). INT training prompted a marked RV dilatation (~26%) but did not further dilate the LV. A reduction in both RV segments deformation in INT rats (apical SR[s^{-1}] -3.3±0.6 vs -3.0±0.4; basal SR[s^{-1}] -3.3±0.7 vs -2.7±0.6; MOD vs INT) led to a decreased global contractile function (dP/dt_{max} [mmHg/ms]: 2.53±0.15 vs 2.17±0.116; MOD vs INT). Echocardiography and hemodynamics consistently pointed to impaired RV diastolic function in INT rats. LV systolic and diastolic functions remained unchanged in all groups. In conclusion, we show a biphasic, unbalanced RV remodeling response with increasing doses of exercise: physiological adaptation after moderate training turns adverse with intensive training, involving disproportionate RV dilatation, decreased contractility and impaired diastolic function. Our findings support the existence of an exercise load threshold beyond which cardiac remodeling becomes maladaptive.

NEW & NOTEWORTHY

Exercise promotes LV eccentric hypertrophy with no changes in systolic or diastolic function in healthy rats. Conversely, RV adaptation to physical activity follows a biphasic, dose-dependent and segmentary pattern. Moderate exercise promotes a mild systolic function enhancement at the RV base, and more intense exercise impairs systolic and diastolic function.

KEY WORDS

Right ventricle; endurance exercise; fibrosis; training load; cardiac remodeling.

GLOSSARY

AW: Anterior wall

CO: Cardiac output

LV: Left ventricle

LVEDD: Left ventricle end-diastolic diameter

LVESD: Left ventricle end-systolic diameter

LVEF: Left ventricle ejection fraction

PW: Posterior wall

RV: Right ventricle

SV: Stroke volume

INTRODUCTION

The beneficial effects of regular physical activity for decreasing the cardiovascular disease burden are well established in the general population and in most patients with heart disease (2, 27). However, the optimal dose of exercise to maximize these benefits is unclear (30, 37). Recent data suggests that the dose-response relationship between the amount of exercise and the incidence of cardiovascular complications follows a U-shaped curve in which some benefits of moderate exercise might be lost at very high training loads (7, 18, 37).

Endurance training requires marked increases in cardiac output (CO) over periods of several hours, thereby superimposing a high degree of stress to all myocardial structures and, particularly, on the right ventricle (RV)(13). Notably, the RV typically works at a low intracavitary pressure at rest under physiological conditions, but pressure dramatically and disproportionally increases during intense exercise (13). This might translate into acute, transient, load-dependent impairment of RV performance after long-term endurance races, as recently described (15, 32, 36). Furthermore, it has been speculated that repetitive insults to the RV could lead to a long-term pathologic RV remodeling, eventually developing a potentially pro-arrhythmogenic substrate in some highly trained athletes (19). In an experimental running rat model, long-term high intensity endurance exercise promoted RV myocardial fibrosis and increased ventricular arrhythmia inducibility in the presence of a relatively preserved LV (3).

While the role of the RV in the development of exercise-induced pathology and on the tolerability of exercise is increasingly being recognized (18), the physiology of RV adaptation to exercise remains largely unknown. Additionally, there is a large inter-individual difference in the degree of RV remodeling both at the global and regional level, where individual athletes show changes that are interpreted as physiological/benign or deleterious for different types of exercise. For example, the basal segment of the RV characteristically dilates and exhibits decreased systolic deformation in most athletes, whereas changes in apical segments show conflicting results (36, 38).

Moreover, little is known about the influence of the training load itself in the segmental RV adaptation.

The present study was designed to assess the influence of training load on global exercise-induced RV remodeling (size, deformation, contractility and filling) as well as on potential different exercise-induced adaptation of the individual RV segments. In order to prevent from confounding factors, we conducted this study in a rat model of long-term endurance exercise at two different exercise intensities (moderate and intense training).

METHODS

Experimental design

This study conformed to the European Community (Directive 86/609/EEC) and Spanish guidelines for the use of experimental animals and was approved by the institutional animal research ethics committee. We used an experimental animal model in which rats were conditioned to run in a treadmill 5 days/week for 16 weeks, as previously described (3, 9). Fifty-five male Wistar rats (200-250g; Charles River Laboratories, France) were randomly assigned to three groups: moderate exercise (MOD, 35cm/s for 45 minutes), high-load exercise (INT, 60cm/s for 1 hour) and age-matched sedentary rats (SED) that served as controls. Estimates from previous studies in rats suggest that these loads approximate 60% and 85% of the maximum oxygen uptake for MOD and INT, respectively (17, 42). The final training load was reached after an initial 2-week adaptation period in which the treadmill speed was progressively increased. Rats were supervised during all training sessions to ensure proper running; animals that did not adapt to the exercise routine were excluded from the study in order to avoid the deleterious effects of physical and psychological stress that could potentially bias our results. All animals were housed in a controlled environment (12/12-hour light/dark cycle) and were provided with *ad libitum* access to food and water. At the end of the training protocol, in vivo right and left ventricular functional and structural remodeling

were assessed in a hemodynamic study and a 2D echocardiogram. In trained rats, the echocardiography and the hemodynamic study were carried out at least 12 hours after the last training session.

Echocardiography

Transthoracic echocardiographic studies were performed at rest in the three groups. The procedure was performed under general anesthesia (isofluorane 2%) and a heating pad, and a phased-array probe 10S (4.5-11.5 Megahertz) attached to a commercially available system (Vivid Q, GE Healthcare Ultrasound, Horten, Norway). The M-mode spectrum was traced in a para-external short axis plane at the level of aortic valve; the RV outflow tract was also measured in this view. Left ventricular (LV) dimensions at both end-diastole (LVEDD) and end-systole (LVESD) were measured at the level of the papillary muscles. The LV anterior (AW) and posterior wall (PW) thickness were measured at end-diastole. LV ejection fraction (EF), fractional shortening (FS), and LV mass were estimated using previously validated formulas in rodents (26, 34):

$$LVEF = \frac{LVEDD^2 - LVESD^2}{LVEDD^2}$$

$$LVFS = \frac{LVEDD - LVESD}{LVEDD} * 100$$

$$LV\ mass = 1.04 * (AW + PW + LVEDD)^3 - LVEDD^3$$

RV end-diastolic (RVEDA) and RV end-systolic areas (RVESA) were measured in an 4-chamber (4C) apical view focusing in the RV; RV fractional area change (RVFAC) was then calculated as (25):

$$RVFAC = \frac{RVEDA - RVESA}{RVEDA} * 100$$

Five consecutive cardiac cycles with color coded Tissue Doppler Imaging (TDI) images were recorded in a 4C apical view and saved for posterior off-line analysis; special care was taken to maintain the Doppler velocity range (0.77 to 46.2 cm/s) as low as possible to avoid aliasing and a

medium frame rate of 250-300 sec. Measurements were calculated as the average of the 5 cardiac cycles. RV segmental deformation was evaluated by strain rate (SR) at basal and apical segments using a sample volume of 2 mm and a specific software package (EchoPac, General Electric Healthcare, Milwaukee, WI, USA). LV and RV diastolic function were estimated by the filling peak velocity (E) of the trans-mitral and trans-tricuspid flow, and mitral septal (e'M) and tricuspid lateral annulus (e'T) velocity during early filling derived from TDI (24). Additionally, isovolumetric relaxation time (IVRT) of both ventricles was evaluated (Figure 1). All cardiac dimensions were body weight-indexed to account for differences in body weight. A LVEDD-to-RVEDA ratio was built to assess the balance between the structural remodeling of the LV and the RV.

Reproducibility was assessed in 12 rats (4 for each study group). Intraobserver and interobserver intraclass correlations were 0.90 and 0.85, respectively, for RV systolic deformation at the basal segment; 0.88 and 0.82 for RV systolic deformation at the apical segment; 0.90 and 0.89 for e' velocity at tricuspid lateral annulus; and 0.88 and 0.85 for e' velocity at septal mitral annulus.

Hemodynamic study

In vivo right and left ventricular contractile remodeling was assessed in an invasive hemodynamic study in a subgroup of rats (16/15/13 for the LV, 8/12/8 for the RV, SED/MOD/INT). Briefly, anesthetized rats (inhaled isoflurane 1.5-2%) were intubated and ventilated (CWE, Ardmore, PA, USA) with parameters recommended by the manufacturer, and kept at 37.0±0.3ºC during the whole experiment with an homeothermic pad (Kent Scientific, USA). RV hemodynamic parameters were first quantified. The right jugular vein was inspected through a <1-cm skin cut at the right aspect of the neck. A 1.9 Fr sensor-tip pressure catheter (Scisence, London, ON, Canada) was inserted through a small incision and gently advanced into the RV. Once a smooth RV pressure curve was obtained, a 10 minute-stabilization period was allowed before data was recorded (PowerLab and Labchart v8.0, AD Instruments). The catheter was thereafter removed, the right jugular vein ligated

and the right carotid exposed. The pressure-tip catheter was thereafter inserted into the right carotid artery and slowly advanced into the left ventricle. Once a smooth left ventricle pressure curve was obtained, a 10 minute-stabilization period was allowed before data was recorded. Data was later analyzed off-line. For both RV and LV recordings, peak systolic and end-diastolic pressure, as well as parameters assessing systolic function (maximum dP/dt) and diastolic function (Tau constant, minimum dP/dt and average dP/dt during isovolumetric relaxation) were quantified (LabChart v8.0. AD Instruments) in 50 consecutive beats and the average calculated for each animal.

In a subgroup of 21 rats (10 SED, 6 MOD, 5 INT), pressure-volume loops were obtained with a conductance pressure-volume catheter and the ADVantage ADV500 system (Transonic, New York, USA). Calibration was conducted as per manufacturer instructions before initiating the procedure. After conventional hemodynamic measurements, the conductance catheter was gently introduced through the right carotid and advanced into the LV. The catheter was carefully mobilized until properly placed (i.e., a smooth sinusoidal curve with phase between 2º and 8º and magnitude between 1400-2600). After a 10-minute stabilization period, simultaneous pressure and volume data was recorded. LV end-diastolic volume (LVEDV) and stroke work were quantified off-line. LV ejection fraction was obtained as:

$$LVEF = \frac{LVEDV - LVESV}{LVEDV} * 100$$

The heart rate was obtained from a single-lead ECG strip recorded during the hemodynamic study.

Wall stress estimation

Wall stress at rest of both ventricles was estimated by mean of hemodynamic and echocardiographic data. To estimate LV wall stress, it was assimilated to an sphere and used a previously described formula (13):

$$LV\ \sigma\ = \frac{LVEDP * LVEDD}{2\ IVS}$$

The particular shape of the RV prevents from reliably fitting it into an sphere without major deviations. We accordingly modelled it as a truncated ellipsoid, and estimated both longitudinal and circular RV wall stress as:

$$RV\ \sigma_{long} = \frac{RVEDP * a^2}{2ch}\left(\frac{bc}{a^2} + \frac{c}{b} - \frac{b}{c}\right)$$

$$RV\ \sigma_{circ} = \frac{RVEDP * c}{2h}\left(\frac{b}{c} + \frac{c}{b} - \frac{bc}{a^2}\right)$$

where:

$$c = \frac{LVEDD}{2}, \qquad a = LVEDL, \qquad h = RVWT$$

$$b = \frac{LVEDD}{2} + SWT + RVEDD$$

Fibrosis assessment

Right ventricular fibrosis was assessed in histological preparations as previously described (3). Briefly, after sacrifice hearts were embedded into paraffin. A basal ventricular section was subsequently obtained and stained with Sirius red staining to identify collagen deposition. A single microphotograph including the whole RV was obtained (Panoramic Desktop, 3DHISTEC, Hungary). Myocardial fibrosis was semi-automatically quantified with ImageJ (NIH, Bethesda, USA) and results given as percentage (%). Perivascular and epicardial fibrosis were excluded from the analysis.

Statistical analysis

Data were analyzed with SPSS Software for Windows (v19.0, IBM, New York, USA). A Gaussian distribution of all continuous variables was confirmed using a Kolmogorov–Smirnov test and values reported as mean±standard error of the mean (SEM). Characteristics of the three groups of rats were

compared by one-way independent ANOVA; if the ANOVA test showed an overall difference, post hoc comparisons were performed with an LSD test. A p-value <0.05 was considered for significance in all analyses.

RESULTS

Two rats in the INT group had to be excluded because of inability to properly complete training sessions; these rats have been excluded from all analyses. All MOD rats finished the experimental protocol. Accordingly, the final population consisted of n=17 for SED, n=19 for MOD, n=17 for INT. The rat characteristics at the end of the experiment are shown in Table 1. Body weight was lower in both trained groups than in sedentary rats. As expected, long-term endurance training induced a significant bradycardia in both MOD and INT groups, with no significant differences between them.

Structural remodeling induced by exercise

The echocardiographic evaluation at rest demonstrated that long-term endurance training promoted remarkable cardiac structural remodeling. In comparison with SED rats, both MOD and INT training induced an enlarged LVEDD and increased LV mass of a similar extent, resulting in a comparable degree of LV eccentric hypertrophy (Table 2 and Figure 2). Invasive volume analyses confirmed a similar LV dilation in both trained groups (MOD, INT) in comparison with sedentary animals (Figure 3A and 3B). Conversely, we found a significant, intensity-dependent RV dilation (Figure 2 and Table 2) which was progressive from SED to MOD (+16% increase in RVEDA) to INT (+26% RVEDA increase) rats. A disproportionate RV dilation in relation to LV size (Figure 4A) translated into a decreased LV-to-RV ratio in the INT group (Figure 4B), thus reinforcing the concept of an unbalanced bi-ventricular structural remodeling in intensively trained individuals.

Systolic functional remodeling induced by exercise

Systolic and diastolic function were evaluated in the resting state through multimodal analyses. Consistent data obtained from echocardiography (Table 2), pressure-volume loop analyses (Figure 3C-D) and intracavitary pressure recordings (Figure 5) demonstrated a virtually unaltered LV systolic function after moderate or intense endurance training in healthy rats. Specifically, LVEF (Table 2 and Figure 3C) and LV maximum dP/dt (Figure 5D) showed similar values across groups.

In contrast, we found marked changes in RV systolic function after physical training. Moderate (MOD) physical activity induced a segment-specific increase in RV deformation: while myocardial deformation increased in the RV apical segment, there were no changes in RV basal segmental deformation (Table 2 and Figure 6). Overall, the global RV systolic function evaluated with FAC was not modified (Table 2). Conversely, RV systolic function was remarkably impaired with the highest training load. Echocardiography displayed a diminished myocardial deformation both in the RV base and apex of the INT group in comparison with MOD (Table 2 and Figure 6). The reduction in myocardial deformation led to a decreased global systolic function as assessed with FAC (Table 2). A lower systolic contractile function of the RV in the INT group was further confirmed in invasive hemodynamic experiments (e.g., decreased dP/dt_{max}, Figure 7).

Diastolic functional remodeling induced by exercise

Exercise did not alter LV filling parameters at rest. Mitral E and e', LV isovolumetric relaxation time (Table 2) and the constant of ventricular relaxation *tau* (Figure 5E), LV minimum dP/dt (Figure 5F) and average dP/dt during isovolumetric relaxation (Figure 5G) were unchanged in all groups.

Similarly, RV diastolic function was unaltered after MOD exercise. Nevertheless, more intense exercise in the INT group prompted a decreased tricuspid E-wave and e' along with a prolonged isovolumetric relaxation time, all these parameters pointing to an impaired RV diastolic

function (Table 2). These data were supported by results from invasive hemodynamic studies showing a prolonged *tau* constant, a decreased RV dP/dt_{min} and average dP/dt during isovolumetric relaxation in INT-trained rats (Figures 6E-G).

Right and left ventricular wall stress at rest

The wall stress estimations at rest for the left and right ventricles are shown in Figure 8. Consistent with a physiological LV remodelling after MOD and INT training, we found no changes in LV wall stress at rest amongst all three groups. Conversely, longitudinal RV wall stress was significantly reduced in MOD-trained rats in comparison to SED; such a reduction was blunted in INT rats. Although it did not reach significance, a similar pattern was found for circular RV wall stress.

Myocardial fibrosis assessment in the RV

Right ventricular fibrosis was assessed in histological preparations. Representative images are shown in Figure 9A. While MOD rats showed a similar fibrosis than SED ones, INT-trained rats developed significantly increased RV myocardial fibrosis (Figure 9B).

DISCUSSION

In the current study, we comprehensively evaluate the structural and functional bi-ventricular cardiac remodeling induced by moderate and intense endurance training in an experimental model. Our results may be summarized in two key findings: a) the pattern of exercise-induced RV remodeling was critically influenced by the training load. While moderate endurance training promoted balanced, harmonic bi-ventricular dilatation along with normal bi-ventricular deformation, contractility and filling, a high training load led to a disproportionate RV dilatation and systo-diastolic functional impairment; b) RV apical and basal segments exhibited different

adaptations to varying intensities of endurance exercise. Our results contribute to the long-debated issue on the role of exercise load in RV remodeling.

Exercise load determines the balance between LV and RV remodeling.

In our study, long-term endurance training of moderate intensity induced a comparable structural remodeling in both ventricles along with an unchanged bi-ventricular diastolic function and an improved RV systolic function. In keeping with recent studies in athletes, moderate endurance training promoted harmonic bi-ventricular dilation (12, 40) and normal bi-ventricular systolic and diastolic function (8, 41). However, it is controversial whether balanced remodeling persists in highly trained individuals. Markedly disproportionate RV structural and functional changes have been shown in some athletes (15, 31), but recent reports have yielded conflicting results and advocated for a balanced bi-ventricular remodeling (5). While small and heterogeneous cohorts and selection biases might explain some of these conflicting results, these differences suggest that large inter-individual responses to exercise exist (16, 36), likely determined by individual predisposition factors and the type and amount of exercise.

Our animal model using individuals with a homogenous genetic background and very controlled exercise regimes overcomes many of these potential biases. Through a multimodal approach including echocardiographic and invasive hemodynamic assessment, our results strongly support that cardiac remodeling after intense physical activity diverges from that of moderate training and is characterized by a disproportionate and dysfunctional RV adaptation.

The RV is particularly sensitive to exercise-induced cardiac remodeling.

Cardiac output is determined by HR and stroke volume (SV), which in turn depends on myocardial deformation and cavity size (4, 28). High intensity endurance exercise requires marked increases in CO over periods of several hours, a requirement that can be reached through an increase in HR, cavity size or myocardial deformation; in most cases, a combination of all them is needed. To accommodate to the high demands of regular exercise, endurance training induces an enlargement

of all cardiac chambers, thus enabling the heart to increase the SV during exercise, at the cost of rising wall stress (10, 28). Altogether, the thin wall of the RV, its geometric shape and the dramatic increase in intracavitary pressure during exercise beget a remarkably high RV workload and make it particularly vulnerable to the undesirable consequences of increased wall stress (13). In our study, a high training load promoted a disproportionate RV dilatation and a decreased RV contractility, as demonstrated by impaired deformation and dP/dt. At rest, mild decreases in RV contractility (13, 20, 21) and a reduced myocardial flow (21) have been claimed to contribute to an enhanced functional and circulatory reserve during exercise in athletes (20). In our work, a very high training load yielded a disproportionate and unbalanced RV enlargement and reduced systolic function at rest, accompanied by an impaired RV diastolic function and fibrosis, suggesting that initial adaptive structural and functional changes become detrimental with certain cumulative training loads. On the other hand, modest changes in LV wall stress during exercise (13) likely account for the lack of a deleterious LV remodeling. Whether myocardial flow is impaired after high training loads remains unknown.

The sort of exercise is an important determinant of cardiac remodeling. In predominantly strength sports (e.g., weight-lifting), exercise bouts are characterized by variable increases in blood pressure, small changes in cardiac output and mild chamber dilation. Conversely, endurance training superimposes a cardiac volume overload that critically determines cardiac remodeling and, likely, contributes to the different response of the LV and RV. In an elegant experimental model of bi-ventricular volume overload, Modesti et al (29) found RV dysfunction and fibrosis with no significant functional or structural changes in the LV. Our results in a transient, repetitive endurance exercise (and thus, volume overload) model, are consistent with their findings. Indeed, we demonstrate RV systo-diastolic dysfunction and fibrosis in the highest exercise load group, while LV function remained unaltered.

We documented an impaired RV diastolic function in intensively trained rats. RV diastolic dysfunction has been shown to fairly predict clinical outcomes in a clinical setting of RV pressure

overload (11), and represents an early sign of RV damage in RV overload experimental models (23, 33). Previous reports from our group documented early signs of RV diastolic dysfunction in a subgroup of high intensity trained endurance athletes (36). However, RV diastolic function in athletes at rest is still a controversial issue (8, 39) and further research is still warranted.

Overall, our data and previous works suggest that RV function is a critical regulator of cardiac performance during exercise bouts. Indeed, recent data from Heiskanen and colleagues (22) showed that exercise capacity in the general population is only determined by RV metabolism, reinforcing that cardiac performance limits are imposed by right-heart characteristics.

Exercise-induced remodeling results in a segmental adaptation of the RV

In our study, myocardial deformation analyses revealed diverging remodeling patterns of the basal and apical segments of the RV through different exercise intensities. Moderate-intensity exercise selectively enhanced apical deformation; intense endurance training, though, blunted such improvement and rendered the apex systolic function similar to that of sedentary animals. Further, intense training associated with an impaired myocardial deformation in the basal segments of the RV. These results are consistent with data in humans reporting a segmentary dysfunction of the basal segment of the RV in athletes (36, 38). Our work suggests that this change is critically governed by training load and supports an exercise load- and segment-dependent RV remodeling after long-term regular training. The causes of this segment-selective remodeling remain unexplored, but it is possible that the heterogeneous morphology of the RV, consisting of a trabeculated apical segment and a smooth and flat inlet segment with a larger capacity, may render the basal segment of the RV more vulnerable to exercise-induced volume overload bouts.

The clinical impact of a decreased RV basal segment deformation in most well-trained individuals is still unclear. In an exercise echocardiography study, La Gerche et al (14) demonstrated a lower RV basal myocardial deformation in athletes at rest, and suggested a role as an adaptive, physiological feature that provides athletes with a larger contractility reserve during

exercise. However, the results obtained through invasive hemodynamics in our animal model question this hypothesis and suggests that intensive training is associated with a true impairment in RV systolic function at rest.

Exercise load determines the sort of cardiac remodeling

Our findings suggest that there is a threshold for training load determined by both intensity and duration beyond which cardiac adaptation might be no longer physiological but rather potentially deleterious, leading to fibrosis and becoming a potential trigger for arrhythmias. This finding further supports the recent notion that the relationship between physical activity load and cardiovascular outcomes follows a U-shaped, rather than lineal, relationship (18).

The mechanisms by which exercise turns deleterious at excessive loads remain obscure. Right ventricular wall stress acutely and linearly increases with exercise intensity (13). It is therefore plausible that low-to-moderate exercise keeps RV wall stress within physiological values while extreme exercise rises it away from a safety range. Similarly, transient systemic inflammation has been found in a dose-dependent way after extenuating exercise bouts. Extrinsic factors such as subclinical myocarditis and performance enhancing drugs have been proposed to contribute to exercise-induced cardiac damage (18).

From a clinical point of view, it would be interesting to identify such a “reversal point”. In our work, we tested only two exercise loads and thereby cannot reliably infer on a specific exercise threshold. Data for exercise-induced atrial fibrillation have suggested a variety of thresholds with potential clinical relevance (1, 6, 18), but these are lacking for the RV. Nevertheless, the ratio between benefits and deleterious consequences of physical activity is likely multifactorial and involves not only the duration and intensity of physical activity, but rather genetic and acquired individual adaptive mechanisms to exercise (18, 36).

Limitations

Some limitations of our work should be acknowledged. First, translation of experimental conclusions to human always warrants caution. It is difficult to estimate how our two different exercise protocols translate into human physical activity. As a rough approximation, if the lifespan of Wistar rats is 2 years, our 18-week exercise protocol (2 weeks of progressive training plus 16 weeks of intensive exercise) would be roughly equivalent to 10 years of daily exercise training in humans. Regarding training load, our intense endurance training has been suggested to correspond to 85% of maximum oxygen uptake (3). We estimate that the moderate training protocol would correspond to a 60% of maximum oxygen uptake (42). Finally, the sedentary group recapitulates a rather extreme form of inactivity; some levels of limited, voluntary exercise would provide a fairer approximation to the lifestyle of most individuals in the general population.

Only young male rats were tested in this study so results might not be extrapolated to females or older age. The effect of stress should always be considered a potential confounder. Nevertheless, maximum efforts were taken to minimize stress responses. Furthermore, we have previously assessed stress levels in INT trained rats and ruled out any significant effects (3). Due to a lower physical demand, we do not expect any significant effect of stress in MOD rats, either.

Finally, most results were obtained under anesthesia. Most anesthetic agents yield some degree of hemodynamic perturbations that could potentially influence our results. Our choice for isoflurane was based on its unique combination of rapid and transient effect with minor hypotensive effects in the absence of exceedingly long exploration times (35).

CONCLUSIONS

In this experimental model of long-term endurance training, exercise load critically determines a biphasic response of the RV performance. Moderate endurance training caused an adaptive RV remodeling characterized by mild RV dilatation and an increase in RV apical deformation. However, vigorous training caused a marked RV remodeling with disproportionate RV dilatation and impaired diastolic and systolic function.

ACKNOWLEDGEMENTS

We thank Mrs. Nadia Castillo for excellent technical assistance.

FUNDING SOURCES: This work was partially funded by grants from the Generalitat de Catalunya (FI-AGAUR 2014-2017, RH040991 to MS), the Spanish Government (Plan Nacional I+D, Ministerio de Economia y Competitividad DEP2010-20565, DEP2013-44923-P and TIN2014-52923-R, cofinanced by the Fondo Europeo de Desarrollo Regional de la Unión Europea "Una manera de hacer Europa" (FEDER), the Instituto de Salud Carlos III (PI13/01580 and PI16/00703) and CIBER CB16/11/00354.

DISCLOSURES: No disclosures to declare

BIBLIOGRAPHY

1. **Aizer A**, **Gaziano JM**, **Cook NR**, **Manson JE**, **Buring JE**, **Albert CM**. Relation of vigorous exercise to risk of atrial fibrillation. *Am J Cardiol* 103: 1572–7, 2009.
2. **Anderson LJ**, **Taylor RS**. Cardiac rehabilitation for people with heart disease: An overview of Cochrane systematic reviews. *Int J Cardiol* 177: 348–361, 2014.
3. **Benito B**, **Gay-Jordi G**, **Serrano-Mollar A**, **Guasch E**, **Shi Y**, **Tardif J-C**, **Brugada J**, **Nattel S**, **Mont L**. Cardiac arrhythmogenic remodeling in a rat model of long-term intensive exercise training. *Circulation* 123: 13–22, 2011.
4. **Bijnens B**, **Cikes M**, **Butakoff C**, **Sitges M**, **Crispi F**. Myocardial Motion and Deformation: What Does It Tell Us and How Does It Relate to Function? *Fetal Diagn Ther* 32: 5–16, 2012.
5. **Bohm P**, **Schneider G**, **Linneweber L**, **Rentzsch A**, **Krämer N**, **Abdul-Khaliq H**, **Kindermann W**, **Meyer T**, **Scharhag J**. Right and Left Ventricular Function and Mass in Male Elite Master Athletes: A Controlled Contrast-Enhanced Cardiovascular Magnetic Resonance Study. *Circulation* 133: 1927–35, 2016.
6. **Calvo N**, **Ramos P**, **Montserrat S**, **Guasch E**, **Coll-Vinent B**, **Domenech M**, **Bisbal F**, **Hevia S**, **Vidorreta S**, **Borras R**, **Falces C**, **Embid C**, **Montserrat JM**, **Berruezo A**, **Coca A**, **Sitges M**, **Brugada J**, **Mont L**. Emerging risk factors and the dose-response relationship between physical activity and lone atrial fibrillation: A prospective case-control study. *Europace* 18: 57–63, 2015.
7. **Calvo N**, **Ramos P**, **Montserrat S**, **Guasch E**, **Coll-Vinent B**, **Domenech M**, **Bisbal F**, **Hevia S**, **Vidorreta S**, **Borras R**, **Falces C**, **Embid C**, **Montserrat JMJM**, **Berruezo A**, **Coca A**, **Sitges M**, **Brugada J**, **Mont L**. Emerging risk factors and the dose-response relationship between physical activity and lone atrial fibrillation: a prospective case-control study. *Europace* 18: 57–63, 2016.

8. **D'Andrea A**, **Riegler L**, **Golia E**, **Cocchia R**, **Scarafile R**, **Salerno G**, **Pezzullo E**, **Nunziata L**, **Citro R**, **Cuomo S**, **Caso P**, **Di Salvo G**, **Cittadini A**, **Russo MG**, **Calabrò R**, **Bossone E**. Range of right heart measurements in top-level athletes: the training impact. *Int J Cardiol* 164: 48–57, 2013.

9. **Fenning A**, **Harrison G**, **Dwyer D**, **Rose'Meyer R**, **Brown L**. Cardiac adaptation to endurance exercise in rats. [Online]. *Mol Cell Biochem* 251: 51–9, 2003. http://www.ncbi.nlm.nih.gov/pubmed/14575304.

10. **Gabrielli L**, **Bijnens BH**, **Butakoff C**, **Duchateau N**, **Montserrat S**, **Merino B**, **Gutierrez J**, **Par?? C**, **Mont L**, **Brugada J**, **Sitges M**, **Paré C**, **Mont L**, **Brugada J**, **Sitges M**. Atrial functional and geometrical remodeling in highly trained male athletes: For better or worse? *Eur J Appl Physiol* 114: 1143–1152, 2014.

11. **Gan CT-J**, **Holverda S**, **Marcus JT**, **Paulus WJ**, **Marques KM**, **Bronzwaer JGF**, **Twisk JW**, **Boonstra A**, **Postmus PE**, **Vonk-Noordegraaf A**. Right Ventricular Diastolic Dysfunction and the Acute Effects of Sildenafil in Pulmonary Hypertension Patients. *Chest* 132: 11–17, 2007.

12. **George KP**, **Warburton DER**, **Oxborough D**, **Scott JM**, **Esch BTA**, **Williams K**, **Charlesworth S**, **Foulds H**, **Oxborough A**, **Hoffman MD**, **Shave R**. Upper limits of physiological cardiac adaptation in ultramarathon runners. *J Am Coll Cardiol* 57: 754–755, 2011.

13. **La Gerche AA**, **Heidbüchel H**, **Burns AT**, **Mooney DJ**, **Taylor AJ**, **Pfluger HB**, **Inder WJ**, **MacIsaac AI**, **Prior DL**, **Heidb??chel H**, **Burns AT**, **Mooney DJ**, **Taylor AJ**, **Pfluger HB**, **Inder WJ**, **MacIsaac AI**, **Prior DL**. Disproportionate exercise load and remodeling of the athlete's right ventricle. *Med Sci Sports Exerc* 43: 974–81, 2011.

14. **La Gerche A**, **Burns AT**, **D'Hooge J**, **Macisaac AI**, **Heidbüchel H**, **Prior DL**. Exercise strain rate imaging demonstrates normal right ventricular contractile reserve and clarifies ambiguous resting measures in endurance athletes. *J Am Soc Echocardiogr* 25: 253–262.e1,

2012.

15. **La Gerche A**, **Burns AT**, **Mooney DJ**, **Inder WJ**, **Taylor AJ**, **Bogaert J**, **MacIsaac AI**, **Heidbüchel H**, **Prior DL**. Exercise-induced right ventricular dysfunction and structural remodelling in endurance athletes. *Eur Heart J* 33: 998–1006, 2012.

16. **La Gerche A**, **MacIsaac AI**, **Burns AT**, **Mooney DJ**, **Inder WJ**, **Voigt J**, **Heidbüchel H**, **Prior DL**. Pulmonary transit of agitated contrast is associated with enhanced pulmonary vascular reserve and right ventricular function during exercise. *J Appl Physiol* 109: 1307–17, 2010.

17. **Guasch E**, **Benito B**, **Qi X**, **Cifelli C**, **Naud P**, **Shi Y**, **Mighiu A**, **Tardif J-C**, **Tadevosyan A**, **Chen Y**, **Gillis M-A**, **Iwasaki Y-K**, **Dobrev D**, **Mont L**, **Heximer S**, **Nattel S**. Atrial fibrillation promotion by endurance exercise: demonstration and mechanistic exploration in an animal model. *J Am Coll Cardiol* 62: 68–77, 2013.

18. **Guasch E**, **Mont L**. Diagnosis, pathophysiology, and management of exercise-induced arrhythmias. *Nat Rev Cardiol* 14: 88–101, 2017.

19. **Heidbüchel H**, **Hoogsteen J**, **Fagard R**, **Vanhees L**, **Ector H**, **Willems R**, **Van Lierde J**. High prevalence of right ventricular involvement in endurance athletes with ventricular arrhythmias. Role of an electrophysiologic study in risk stratification. *Eur Heart J* 24: 1473–80, 2003.

20. **Heinonen I**, **Kudomi N**, **Kemppainen J**, **Kiviniemi A**, **Noponen T**, **Luotolahti M**, **Luoto P**, **Oikonen V**, **Sipilä HT**, **Kopra J**, **Mononen I**, **Duncker DJ**, **Knuuti J**, **Kalliokoski KK**. Myocardial blood flow and its transit time, oxygen utilization, and efficiency of highly endurance-trained human heart. *Basic Res Cardiol* 109: 413, 2014.

21. **Heinonen I**, **Nesterov S V.**, **Liukko K**, **Kemppainen J**, **Någren K**, **Luotolahti M**, **Virsu P**, **Oikonen V**, **Nuutila P**, **Kujala UM**, **Kainulainen H**, **Boushel R**, **Knuuti J**, **Kalliokoski KK**. Myocardial blood flow and adenosine A2A receptor density in endurance athletes and untrained men. *J Physiol* 586: 5193–202, 2008.

22. **Heiskanen MA**, **Leskinen T**, **Eskelinen J-J**, **Heinonen IHA**, **Löyttyniemi E**, **Virtanen K**, **Pärkkä JP**, **Hannukainen JC**, **Kalliokoski KK**. Different Predictors of Right and Left Ventricular Metabolism in Healthy Middle-Aged Men. *Front Physiol* 6: 389, 2015.

23. **Hessel MHM**, **Steendijk P**, **den Adel B**, **Schutte CI**, **van der Laarse A**. Characterization of right ventricular function after monocrotaline-induced pulmonary hypertension in the intact rat. *AJP Hear Circ Physiol* 291: H2424–H2430, 2006.

24. **Lang RM**, **Badano LP**, **Mor-Avi V**, **Afilalo J**, **Armstrong A**, **Ernande L**, **Flachskampf F a**, **Foster E**, **Goldstein S a**, **Kuznetsova T**, **Lancellotti P**, **Muraru D**, **Picard MH**, **Rietzschel ER**, **Rudski L**, **Spencer KT**, **Tsang W**, **Voigt J-U**. Recommendations for cardiac chamber quantification by echocardiography in adults: an update from the American Society of Echocardiography and the European Association of Cardiovascular Imaging. *Eur Heart J Cardiovasc Imaging* 16: 233–70, 2015.

25. **Lawrence G Rudski MD FC**, **Wyman W Lai MD MPHF**, **Jonathan Afilalo MD M**, **Lanqi Hua RDCS F**, **BSc MDH**, **Krishnaswamy Chandrasekaran MD F**, **Md SDS**, **Md EKL**, **Md NBS**. Guidelines for the Echocardiographic Assessment of the Right Heart in Adults: A Report from the American Society of Echocardiography. *J Am Soc Echocardiogr* 23: 685–713, 2010.

26. **Litwin SE**, **Katz SE**, **Weinberg EO**, **Lorell BH**, **Aurigemma GP**, **Douglas PS**. Serial Echocardiographic-Doppler Assessment of Left Ventricular Geometry and Function in Rats With Pressure-Overload Hypertrophy : Chronic Angiotensin-Converting Enzyme Inhibition Attenuates the Transition to Heart Failure. *Circulation* 91: 2642–2654, 1995.

27. **Loef M**, **Walach H**. The combined effects of healthy lifestyle behaviors on all cause mortality: A systematic review and meta-analysis. *Prev Med (Baltim)* 55: 163–170, 2012.

28. **Marciniak A**, **Claus P**, **Sutherland GR**, **Marciniak M**, **Karu T**, **Baltabaeva A**, **Merli E**, **Bijnens B**, **Jahangiri M**. Changes in systolic left ventricular function in isolated mitral regurgitation. A strain rate imaging study. *Eur Heart J* 28: 2627–2636, 2007.

29. **Modesti PA**, **Vanni S**, **Bertolozzi I**, **Cecioni I**, **Lumachi C**, **Perna AM**, **Boddi M**, **Gensini GF**. Different Growth Factor Activation in the Right and Left Ventricles in Experimental Volume Overload. *Hypertension* 43: 101–108, 2004.

30. **O'Keefe JH**, **Lavie CJ**. Run For Your Life...At a Comfortable Speed And Not Too Far. *Heart* 99: 516–520, 2012.

31. **Oxborough D**, **Sharma S**, **Shave R**, **Whyte G**, **Birch K**, **Artis N**, **Batterham AM**, **George K**. The right ventricle of the endurance athlete: the relationship between morphology and deformation. *J Am Soc Echocardiogr* 25: 263–71, 2012.

32. **Oxborough D**, **Shave R**, **Warburton D**, **Williams K**, **Oxborough A**, **Charlesworth S**, **Foulds H**, **Hoffman MD**, **Birch K**, **George K**. Dilatation and dysfunction of the right ventricle immediately after ultraendurance exercise: exploratory insights from conventional two-dimensional and speckle tracking echocardiography. *Circ Cardiovasc Imaging* 4: 253–63, 2011.

33. **Reddy S**, **Zhao M**, **Hu D-Q**, **Fajardo G**, **Katznelson E**, **Punn R**, **Spin JM**, **Chan FP**, **Bernstein D**. Physiologic and molecular characterization of a murine model of right ventricular volume overload. *AJP Hear Circ Physiol* 304: H1314–H1327, 2013.

34. **Reffelmann T**, **Kloner RA**. Transthoracic echocardiography in rats. Evalution of commonly used indices of left ventricular dimensions, contractile performance, and hypertrophy in a genetic model of hypertrophic heart failure (SHHF-Mcc-facp-Rats) in comparison with Wistar rats during. *Basic Res Cardiol* 98: 275–84, 2003.

35. **Sano Y**, **Ito S**, **Yoneda M**, **Nagasawa K**, **Matsuura N**, **Yamada Y**, **Uchinaka A**, **Bando YK**, **Murohara T**, **Nagata K**. Effects of various types of anesthesia on hemodynamics, cardiac function, and glucose and lipid metabolism in rats. *Am J Physiol Heart Circ Physiol* 311: H1360–H1366, 2016.

36. **Sanz de la Garza M**, **Grazioli G**, **Bijnens BH**, **Pajuelo C**, **Brotons D**, **Subirats E**, **Brugada R**, **Roca E**, **Sitges M**. Inter-individual variability in right ventricle adaptation after

an endurance race. *Eur J Prev Cardiol* 23: 1114–24, 2015.

37. **Schnohr P**, **O'Keefe JH**, **Marott JL**, **Lange P**, **Jensen GB**. Dose of jogging and long-term mortality: The Copenhagen City heart study. *J Am Coll Cardiol* 65: 411–419, 2015.

38. **Teske AJ**, **Prakken NH**, **De Boeck BW**, **Velthuis BK**, **Martens EP**, **Doevendans PA**, **Cramer MJ**. Echocardiographic tissue deformation imaging of right ventricular systolic function in endurance athletes. *Eur Heart J* 30: 969–77, 2009.

39. **Teske AJ**, **Prakken NH**, **De Boeck BWL**, **Velthuis BK**, **Doevendans PA**, **Cramer MJM**. Effect of Long Term and Intensive Endurance Training in Athletes on the Age Related Decline in Left and Right Ventricular Diastolic Function as Assessed by Doppler Echocardiography. *Am J Cardiol* 104: 1145–1151, 2009.

40. **Utomi V**, **Oxborough D**, **Ashley E**, **Lord R**, **Fletcher S**, **Stembridge M**, **Shave R**, **Hoffman MD**, **Whyte G**, **Somauroo J**, **Sharma S**, **George K**. Predominance of normal left ventricular geometry in the male "athlete"s heart'. *Heart* 100: 1264–71, 2014.

41. **Utomi V**, **Oxborough D**, **Ashley E**, **Lord R**, **Fletcher S**, **Stembridge M**, **Shave R**, **Hoffman MD**, **Whyte G**, **Somauroo J**, **Sharma S**, **George K**. The impact of chronic endurance and resistance training upon the right ventricular phenotype in male athletes. *Eur J Appl Physiol* 115: 1673–82, 2015.

42. **Wisløff U**, **Helgerud J**, **Kemi OJ**, **Ellingsen O**. Intensity-controlled treadmill running in rats: VO(2 max) and cardiac hypertrophy. *Am J Physiol Heart Circ Physiol* 280: H1301-10, 2001.

560 **Table 1: Population characteristics and echocardiographic parameters in moderate and**

561 **intense training groups and controls.**

	SED (N=17)	**MOD** (N=19)	**INT** (N=17)	**ANOVA (p)**
Weight (g)	503±20	416±9*	409±10*	**<0.01**
HR (beats/min)	380±4	364±7*	349±8*	**<0.01**

562

563

564 **Table 2: Echocardiographic parameters at the end of the experimental protocol in all animals.**

565 **RVEDA:** right ventricle end-diastolic area; **RVOT:** right ventricle outflow tract; **RVFAC:** right

566 ventricle fractional area change; **SR:** strain rate; **RVIRT/LVIRT:** right/left ventricle isovolumetric

567 relaxation time; **LVEDD**: left ventricle end diastolic diameter; AW: left ventricle anterior wall;

568 **LVEF:** left ventricle ejection fraction; **LVFS:** left ventricle fractional shortening. *p<0.05 vs SED;

569 † p<0.05 vs MOD.

	SED (N=17)	**MOD (N=19)**	**INT (N=17)**	**ANOVA (p)**
Left ventricle dimensions and function				
LVEDD (mm/Kg)	15.35±0.51	18.32±0.35*	18.51±0.40*	**<0.01**
LVEDD (mm)	7.54±0.22	7.51±0.31	7.50±0.34*	**0.66**
LV mass (g/Kg)	1.17±0.05	1.38±0.04*	1.44±0.05*	**<0.01**
LV mass (mg)	577.8±60	572.8±80	583.4±61	**0.89**
AW/LVEDD	0.16±0.01	0.16±0.01	0.16±0.02	**0.29**
LVEF (%)	66.6±0.60	65.3±0.48	65.2±0.60	**0.38**
LVFS (%)	41.9±0.52	41.2±0.41	41.0±0.51	**0.37**
E mitral (cm/s)	0.85±0.02	0.85±0.02	0.86±0.02	**0.89**
e' mitral (mm/s)	3.98±0.15	4.20±0.15	4.40±0.13	**0.17**
LVIRT / HR ((ms*min/beats)x100)	4.7±0.24	5.0±0.25	5.2±0.26	**0.32**
Right ventricle dimensions and function				
RVEDA (mm^2/Kg)	69.51±8.8	80.42±9.6*	88.0 ± 9.2*†	<0.01
RVEDA (mm2)	34.4±4.0	33.3±3.7	35.7±2.4	0.10
RVOT (mm/Kg)	7.52±0.27	8.83±0.19*	9.05±0.25*	<0.01
RVOT (mm)	2.83±0.15	2.75±0.11	2.81±0.17	0.19
RVFAC (%)	42.92±1.20	42.34±0.60	40.01±1.02	0.09
RV apical free wall SR (s^{-1})	2.83±0.14	3.33±0.15*	3.01±0.10	0.04
RV basal free wall SR (s^{-1})	3.29±0.24	3.28±0.17	2.71±0.14*†	0.04

E tricuspid (cm/s)	0.75±0.03	0.75±0.02	0.64±0.02*†	<0.01
e' tricuspid (mm/s)	4.20±0.18	4.10±0.13	3.30±0.13*†	<0.01
RVIRT / HR ((ms*min/beats)x100)	4.20±0.27	4.26±0.25	5.27±0.39*	0.03

570

571

FIGURE LEGENDS

Figure 1: Quantification of left and right ventricle isovolumetric relaxation time (L/RVIRT). (A) LVIRT was calculated in an apical 5-chamber view where both continuous-wave Doppler at the conjunction of the LV inflow and outflow was recorded; the result was corrected by the R-R interval. (B) To quantify RVIRT, recordings from two different images were used: Pulsed-wave Doppler (PW) at RV outflow tract in a parasternal short axis view, and PW at tricuspid valve in an apical 4-chamber view. Then, RVIRT was calculated as: (time from the R wave of QRS to triscuspid valve opening [TVO]) – (time from R wave of QRS to pulmonary valve clousure [PVC]). In both cases, the average of 5 consecutive cardiac cycles was calculated.

Figure 2: Echocardiographic assessment of LV and RV size in the three study groups: Upper panel: representative echocardiographic images of all groups. The RV end-diastolic area has been highlighted. Lower panel: quantification (mean±SEM) of LV and RV size in all groups. While LV size was similar in MOD and INT groups, RV size in the INT group was larger than in MOD. SED: sedentary; MOD: moderate training; INT: intense training; LVEDD: LV end diastolic diameter; RVEDA: RV end diastolic area. Omnibus test for both LVEDD and RVEDA $p<0.0001$.

Figure 3: Pressure-volume loop analyses in the LV in all groups. (A) Representative examples for each of the SED, MOD and INT groups. (B-D) Parameters analyzed in this experiment, showing LV end-diastolic volume (B), LV ejection fraction (C) and stroke work (D). Omnibus tests: LVEDV $p=0.004$; LVEF $p=0.98$; SW $p=0.41$. *$p<0.05$

Figure 4: Assessment of LV to RV size correlation and ratio. (A) Correlation between LV size (LVEDD in X-axis) and RV size (RVEDA in Y-axis). Mean±SEM is shown for each group. (B) LV-to-RV ratio data (Tukey Boxplot) showed a significant imbalance in RV size in the INT group, denoting disproportionate RV size. Omnibus test for LV-RV ration $P=0.049$. *$p<0.05$

Figure 5: Left ventricle hemodynamic parameters in the three study groups. (A) Representative recordings of LV in all groups, showing an ECG (upper panel), LV pressure curve

(middle panel) and derived LV dP/dt (lower panel). (B-G) Results for LV hemodynamic parameters: systolic pressure (LVSP) (B), end-diastolic pressure (LVEDP) (C), maximum dP/dt (D), *Tau* constant (E), minimum dP/dt (F) and average dP/dt during isovolumetric relaxation (IRP dP/dt) (G). Omnibus tests: LVSP p=0.53; LVEDP p=0.21; LV dP/dt_{max} p=0.16; LV tau p=0.72; LV dP/dt_{min} p=0.37; IRP dP/dt p=0.66.

Figure 6: Right ventricle function evaluated by 2D-echocardiography and color-coded Tissue Doppler Imaging (TDI) in the three study groups. Strain rate TDI values (mean±SEM) for the three study groups. RV apical deformation improves with moderate training, but regresses and RV basal deformation is impaired after intense training. SED: sedentary; MOD: moderate training; INT: intense training; SR: Strain rate. Omnibus test: RV Apex SR p=0.032; RV Base SR p=0.043.

Figure 7: Right ventricle hemodynamic parameters in the three study groups. (A) Representative recordings in all groups, showing and ECG (upper panel), RV pressure curve (middle panel) and derived RV dP/dt (lower panel). (B-G) Results for RV hemodynamic parameters: systolic pressure (RVSP) (B), end-diastolic pressure (RVEDP) (C), maximum dP/dt (D), *Tau* constant (E), minimum dP/dt (F) and average dP/dt during isovolumetric relaxation (IRP dP/dt) (G). Omnibus tests: RVSP p=0.19; RVEDP p=0.41; RV dP/dt_{max} p=0.046; RV tau p=0.035; RV dP/dt_{min} p=0.04; IRP dP/dt p=0.034. *p<0.05.

Figure 8: Estimation of wall stress in both ventricles. Data is shown for the left ventricle (LV, left panel; omnibus test p=0.28), the longitudinal RV wall stress ($RV\sigma_{long}$, middle panel, omnibus test p=0.03) and the circular RV wall stress ($RV\sigma_{circ}$, right panel, omnibus test p=0.18) *p<0.05.

Figure 9: Right ventricular fibrosis in the three study groups. (A) Representative images of Sirius red-stained samples of the RV of the SED, MOD and INT groups. (B) Myocardial fibrosis quantification (Omnibus test p=0.02). Bar=100µm. *p<0.05; **p<0.01

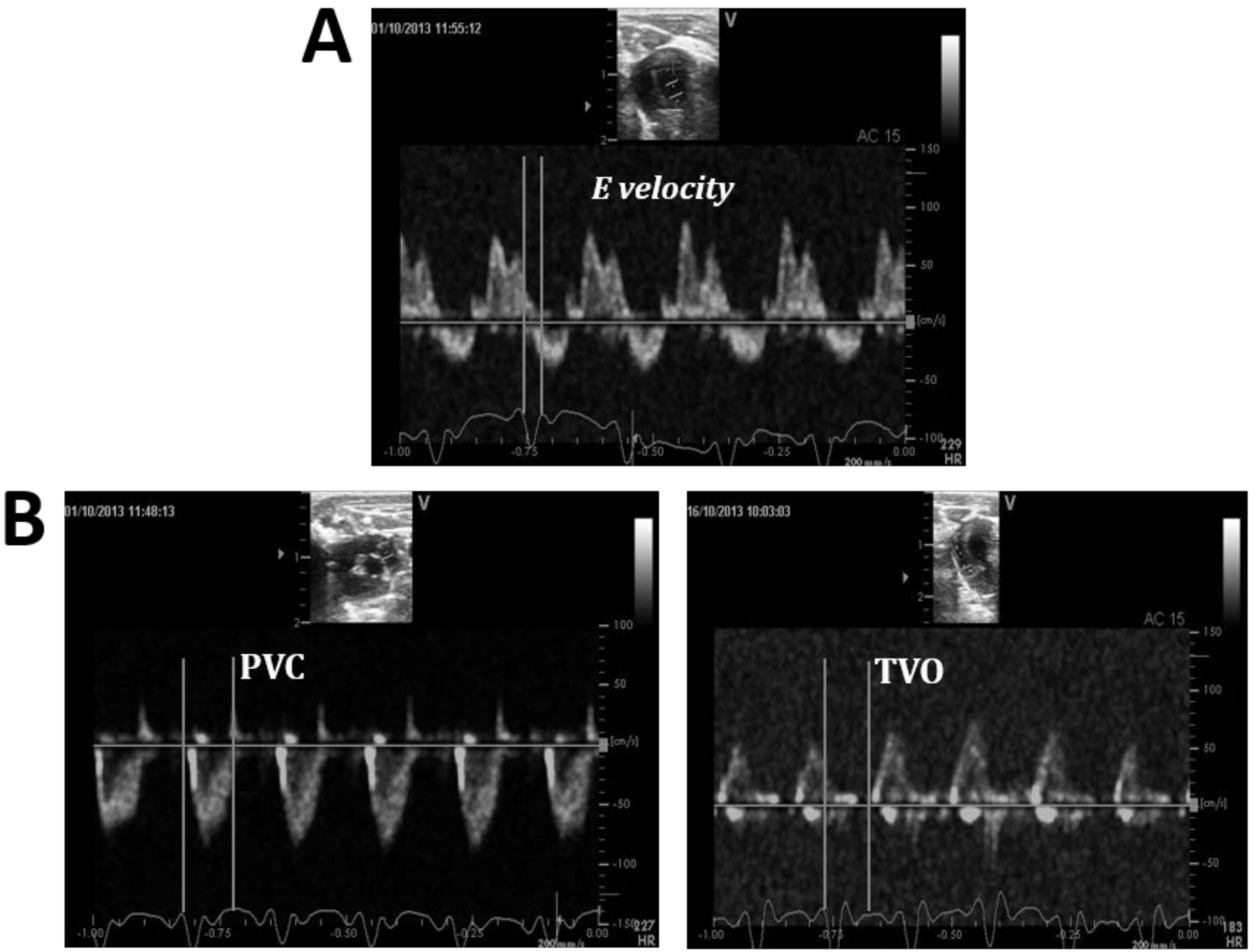
A
01/10/2013 11:55:12
V
AC 15
E velocity
150
100
50
[cm/s]
-50
-100
-1.00
-0.75
-0.50
-0.25
0.00
229
HR
B
01/10/2013 11:48:13
V
PVC
100
50
[cm/s]
-50
-100
-150
227
HR
16/10/2013 10:03:03
V
AC 15
TVO
150
100
50
[cm/s]
-50
-100
183
HR

Figure 1


SED
MOD
INT

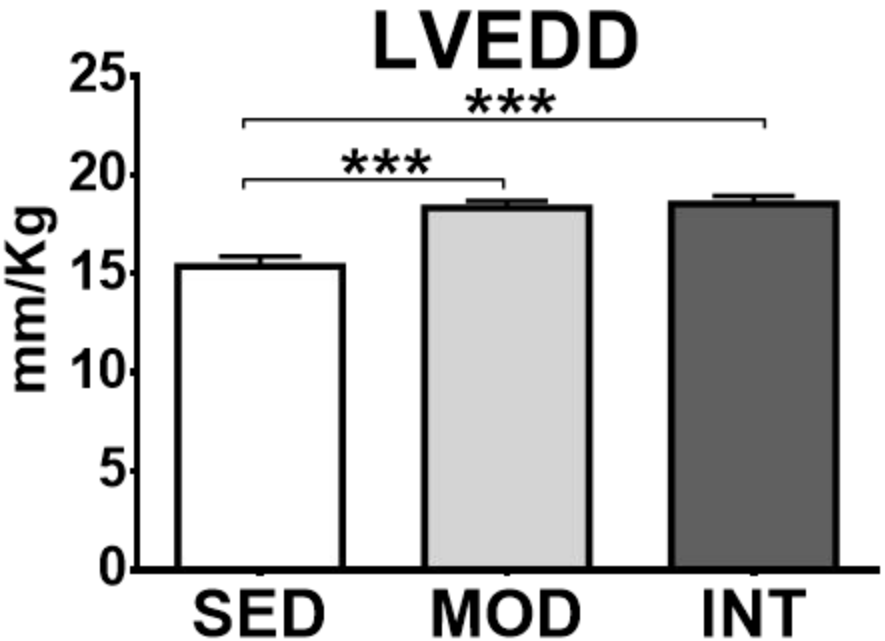
LVEDD
25
20
15
10
5
0
mm/Kg
***
***
SED
MOD
INT

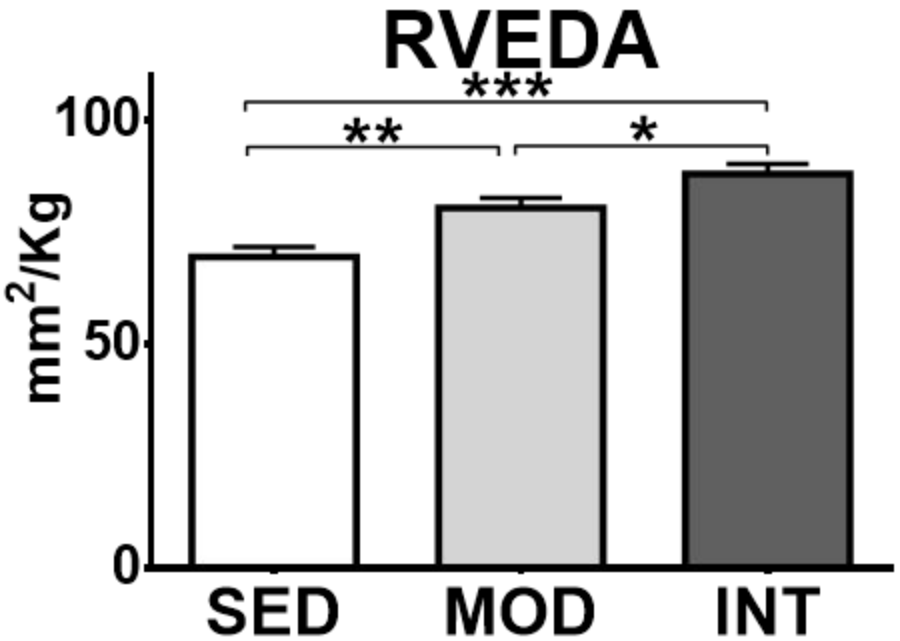
RVEDA
100
50
0
mm²/Kg
***
**
*
SED
MOD
INT

Figure 2

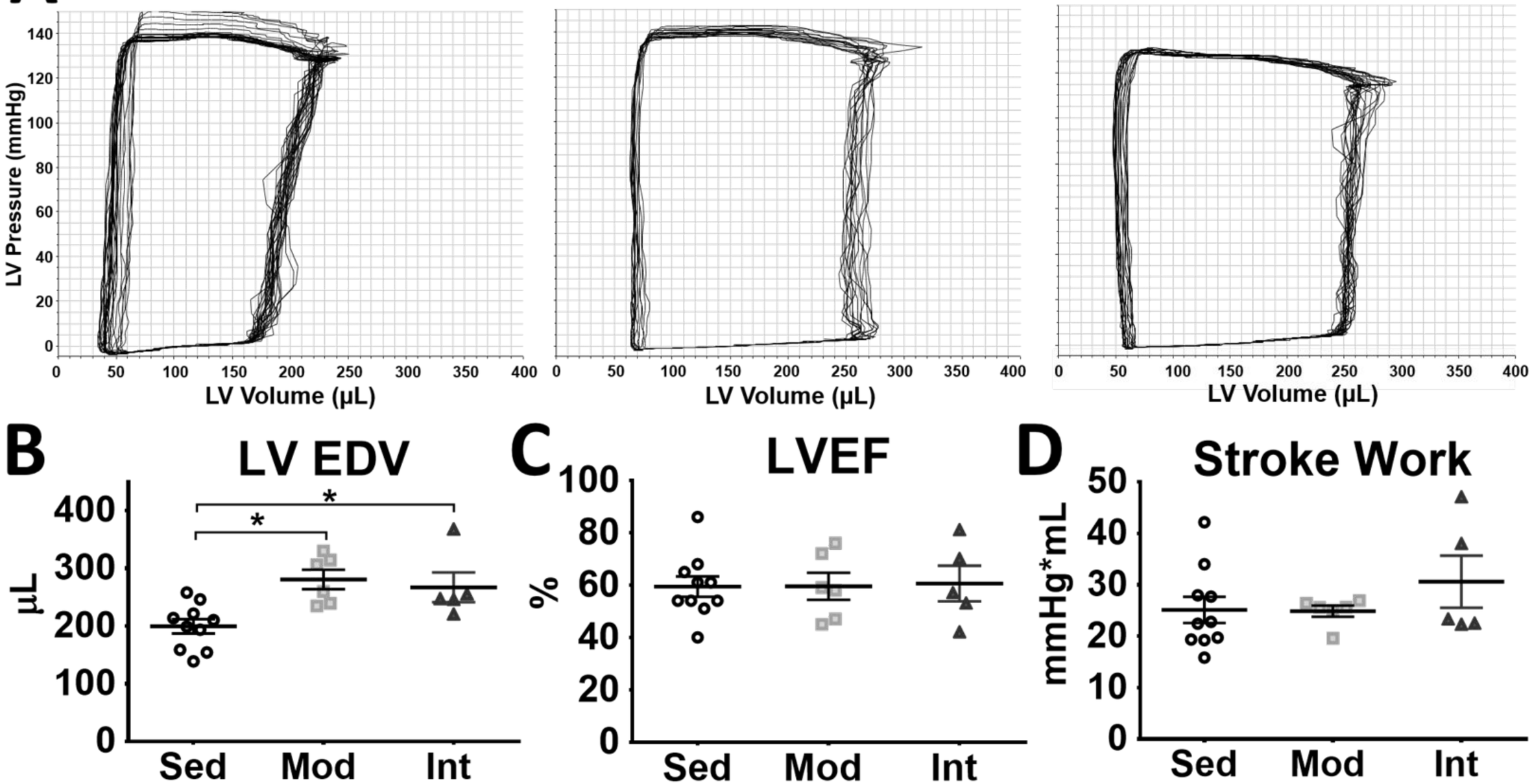
A
SED
MOD
INT
LV Pressure (mmHg)
LV Volume (µL)
B
LV EDV
µL
Sed
Mod
Int
C
LVEF
%
D
Stroke Work
mmHg*mL

Figure 3

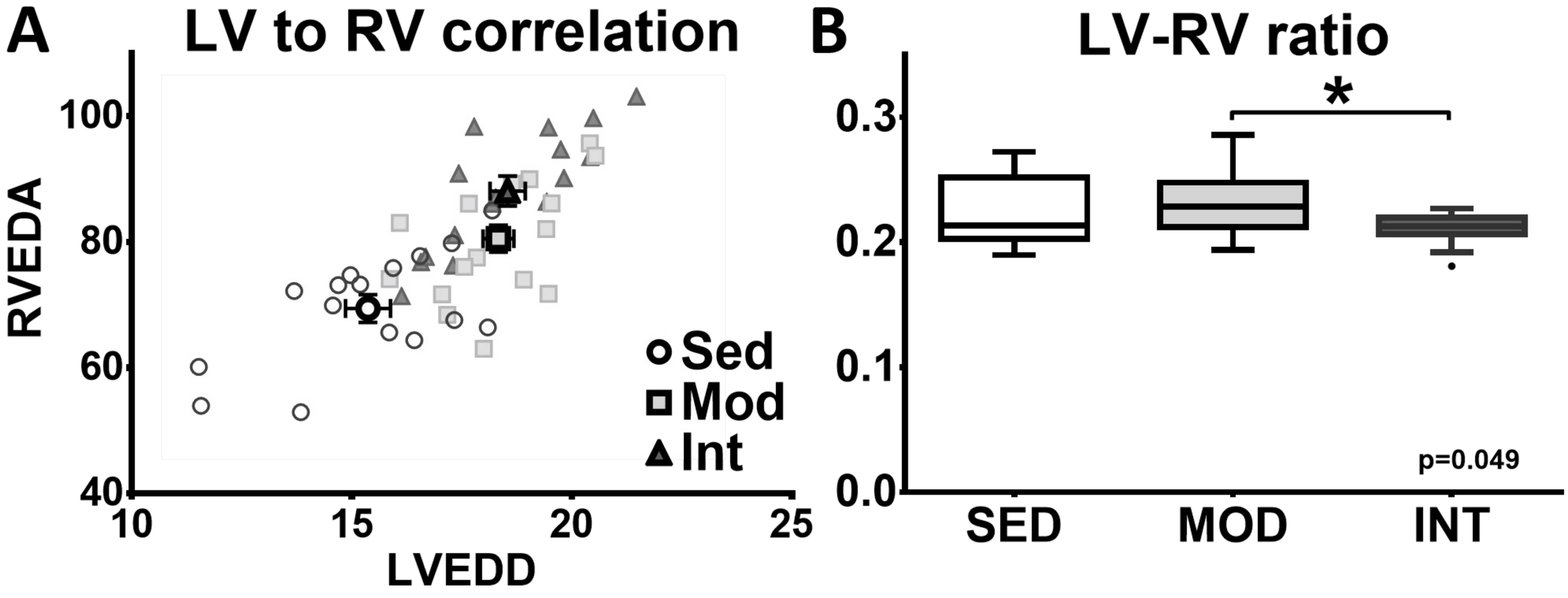
A
LV to RV correlation
RVEDA
LVEDD
100
80
60
40
10
15
20
25
Sed
Mod
Int
B
LV-RV ratio
0.3
0.2
0.1
0.0
*
p=0.049
SED
MOD
INT

Figure 4

Left Ventricle hemodynamics

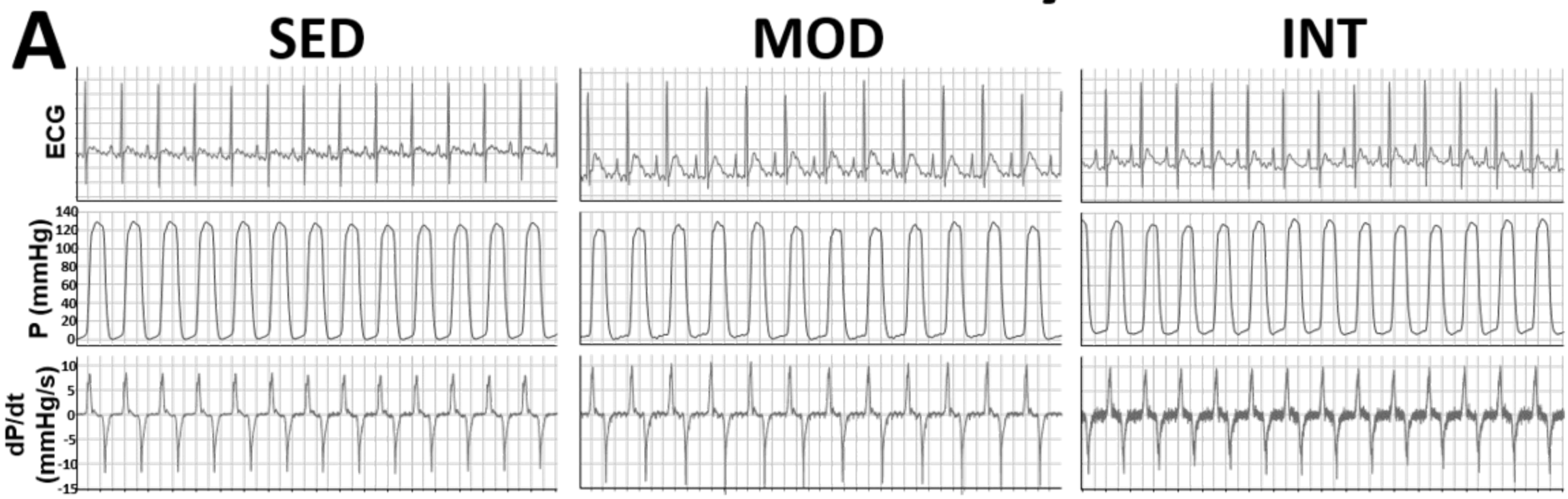

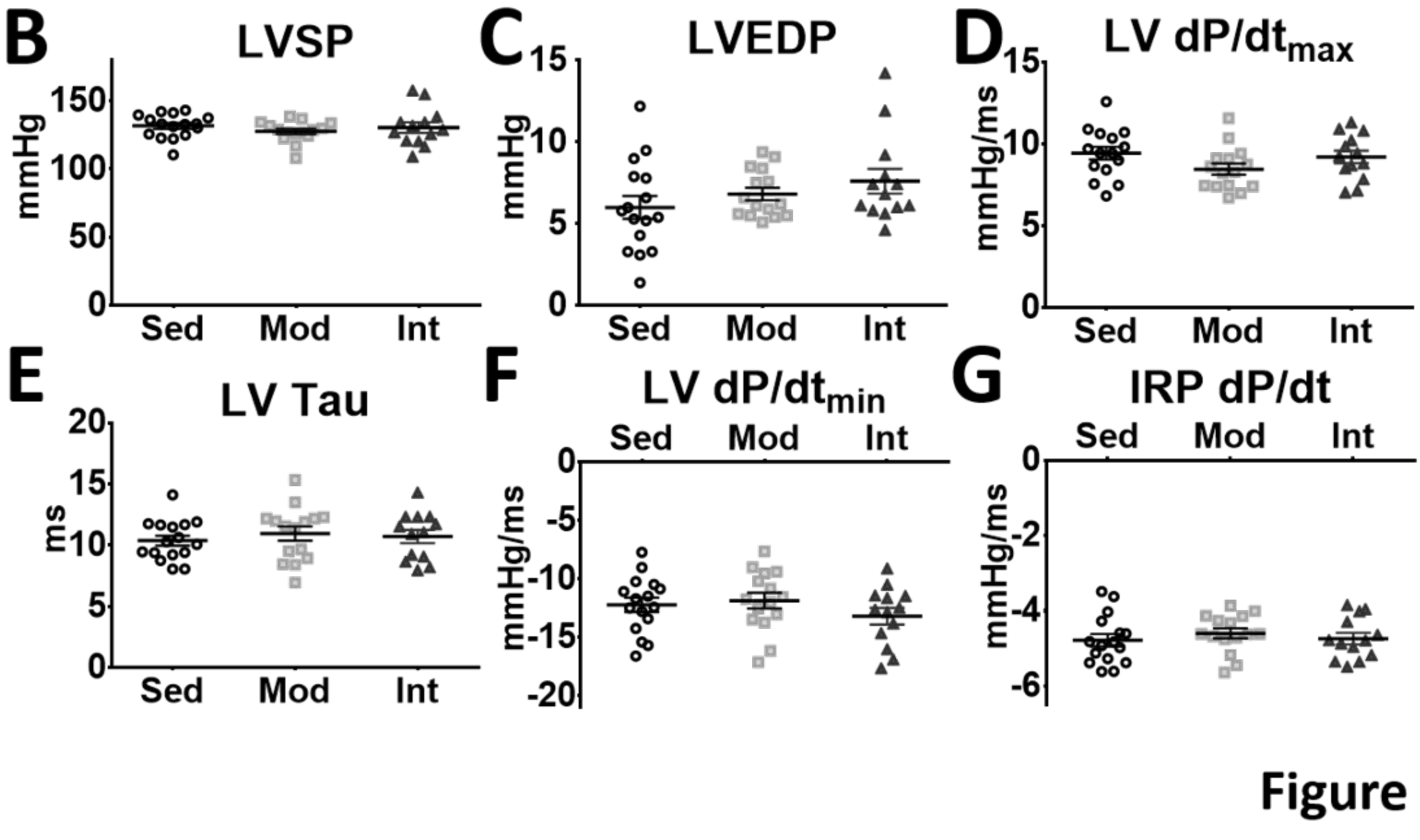

Figure 5

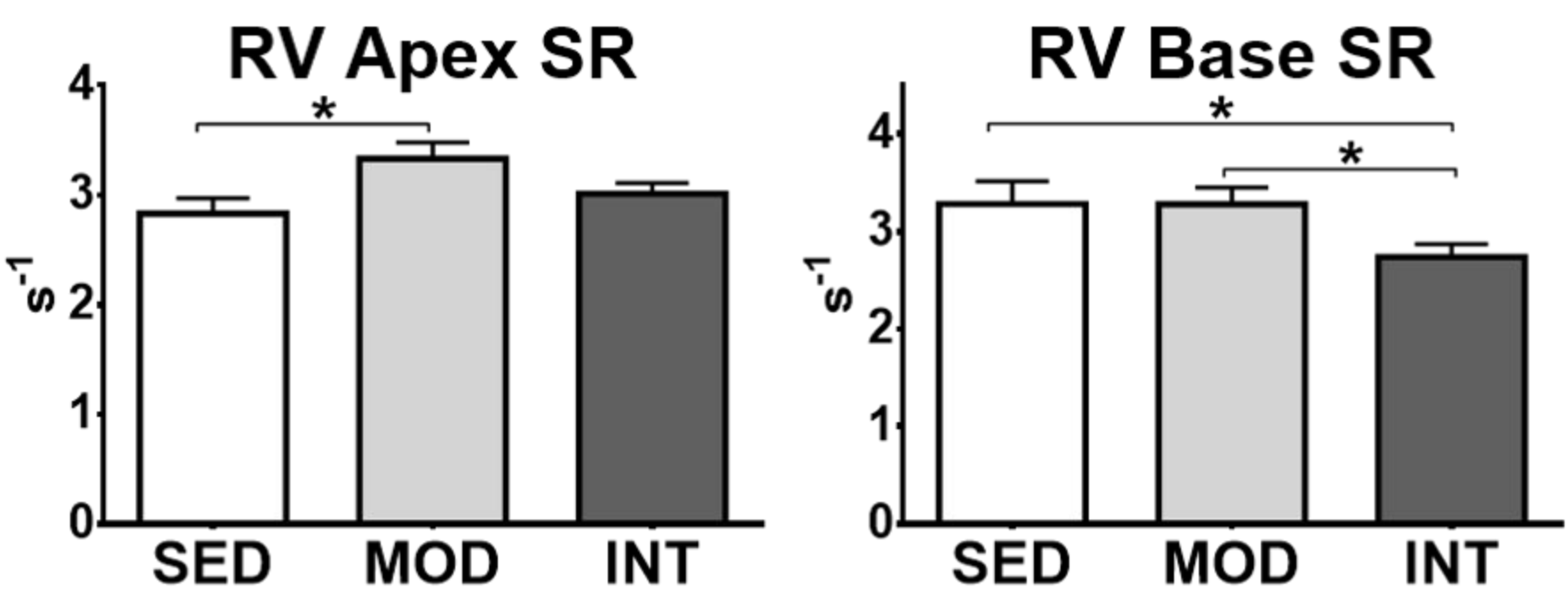

Figure 6

Right Ventricle hemodynamics

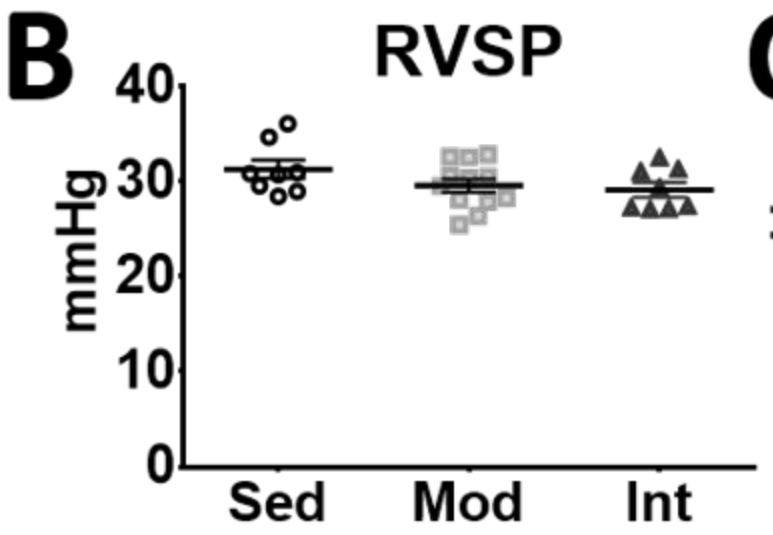

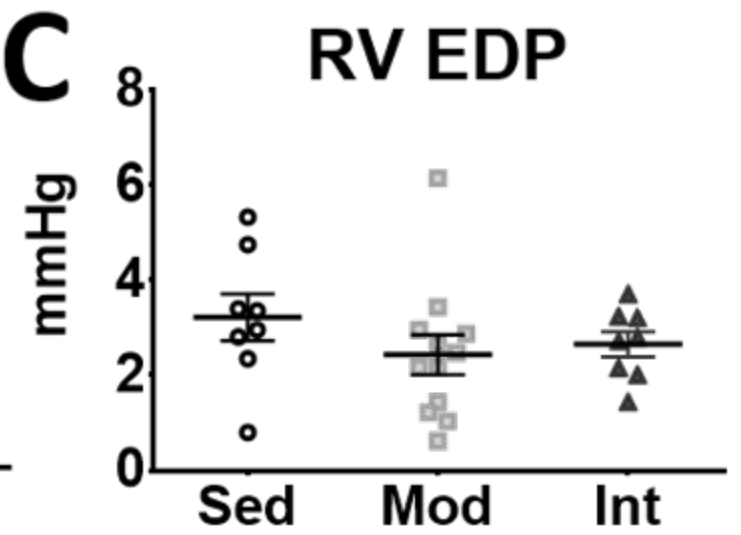

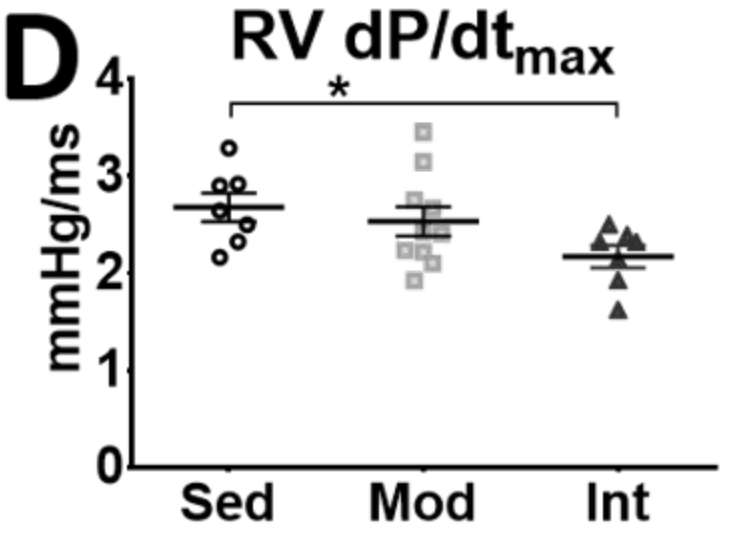

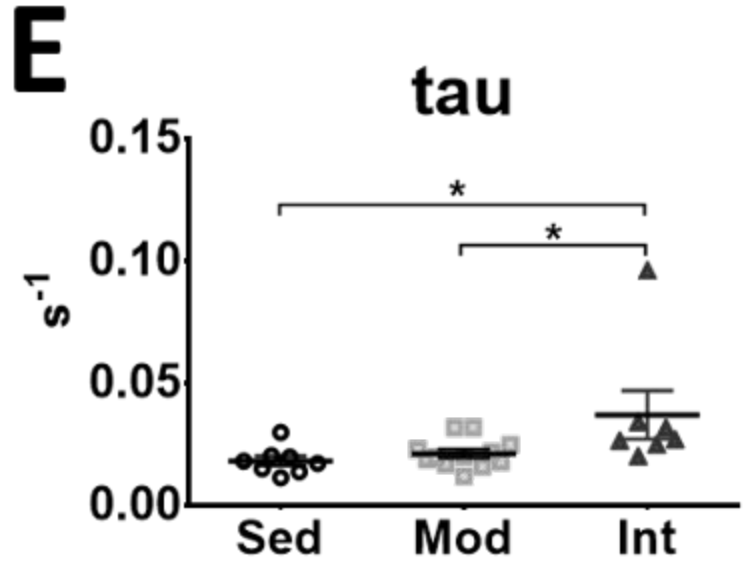

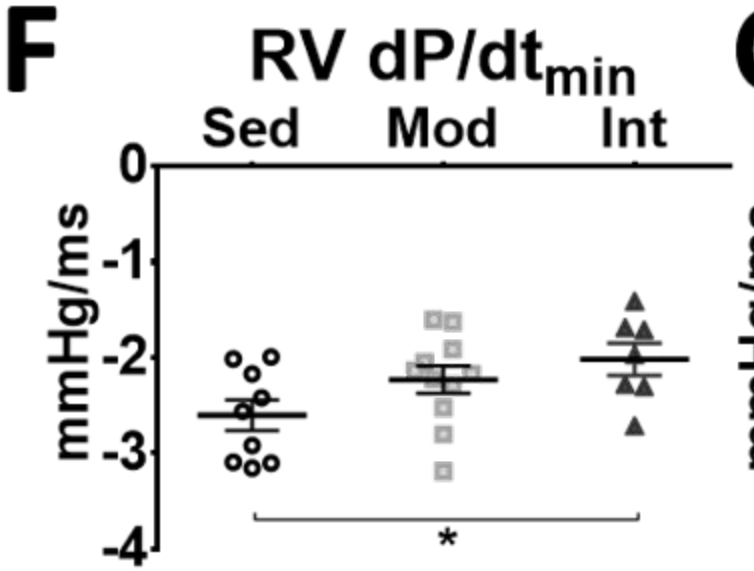

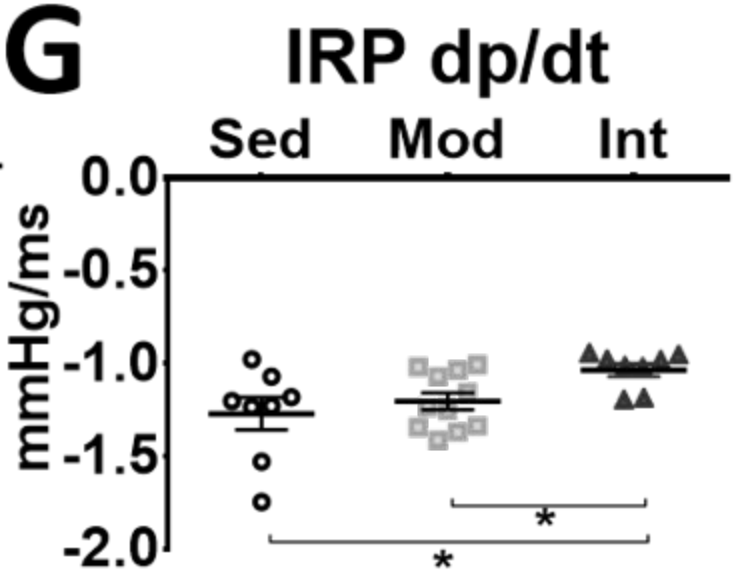

Figure 7

Wall stress estimation

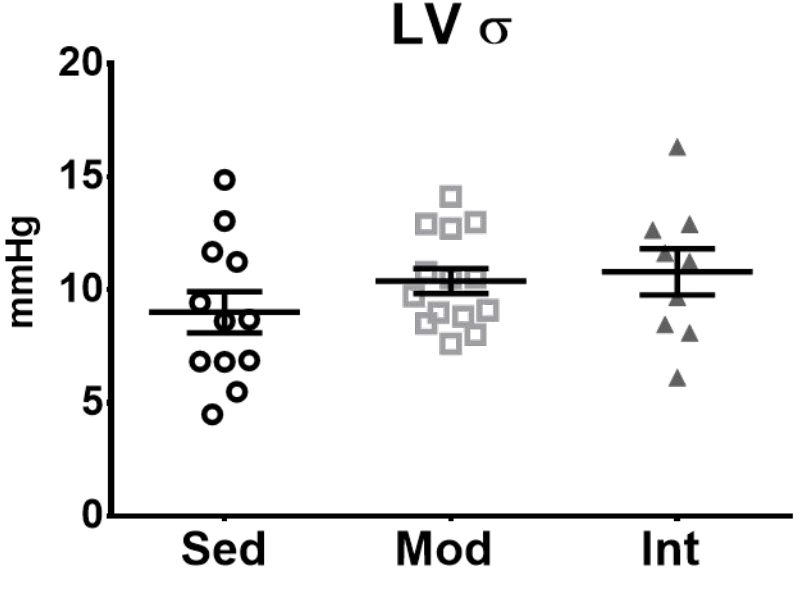

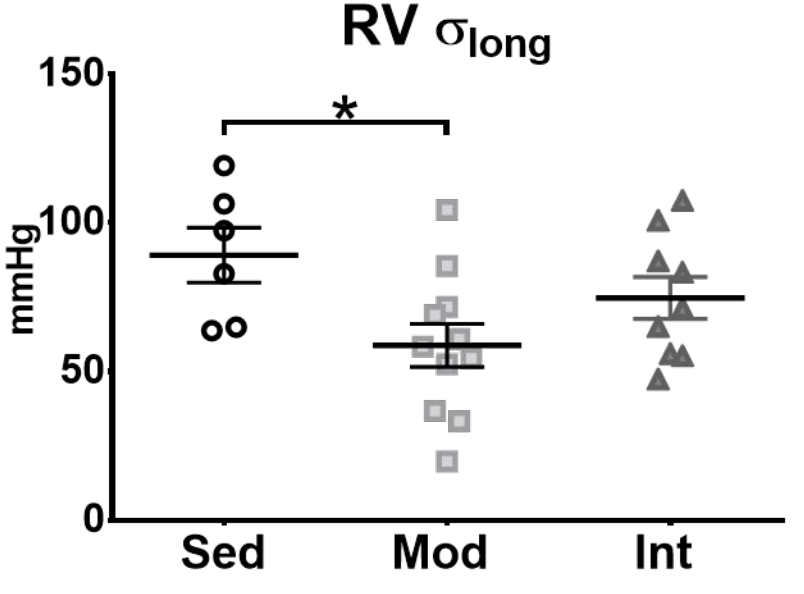

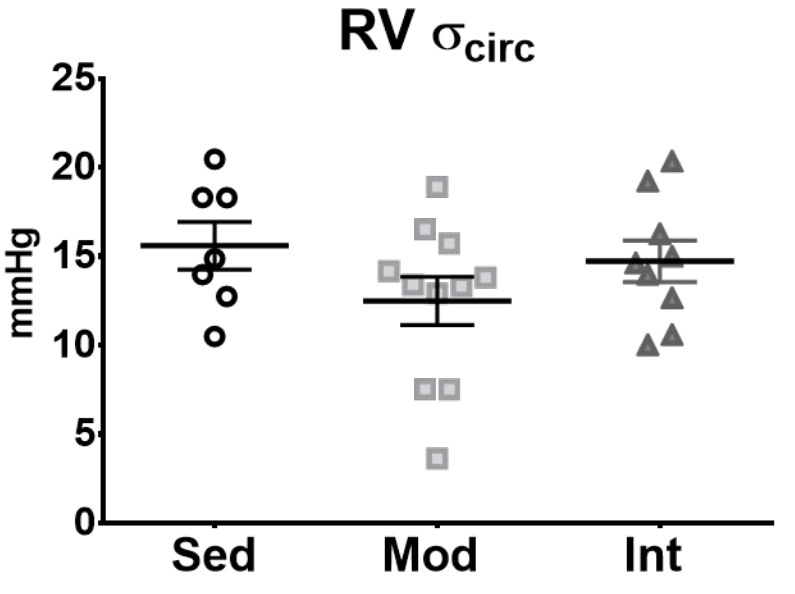

Figure 8

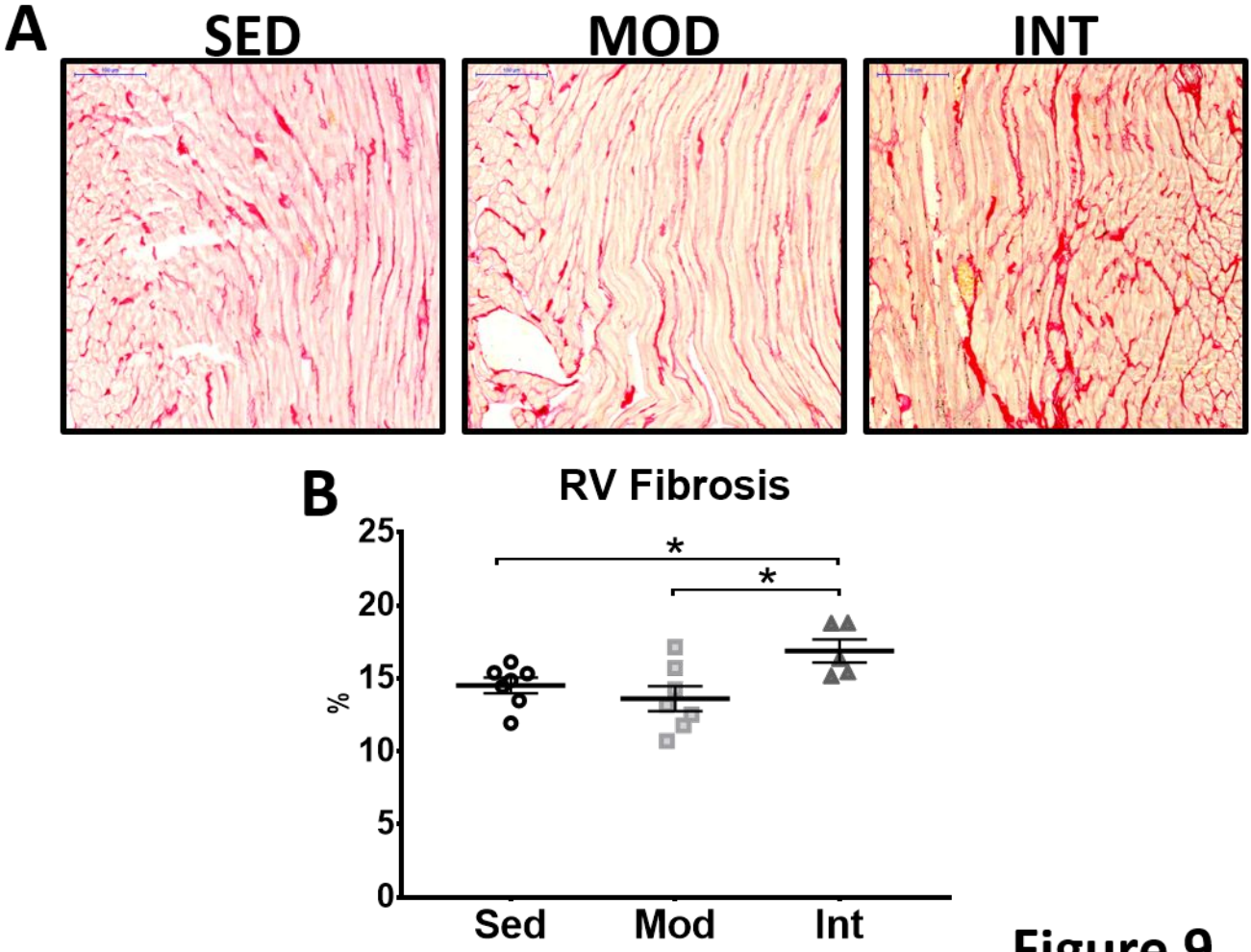

Figure 9